Available online at www.sciencedirect.com

ScienceDirect

Nuclear and Particle Physics Proceedings 318–323 (2022) 22–26

www.elsevier.com/locate/nppp

Recent Jet Measurements in ALICE *

Hannah Bossi for the ALICE Collaboration [a,**]

[a] *Yale University, Wright Laboratory, New Haven, CT, USA*

Abstract

The precise measurement of jets in pp collisions plays a critical role in the study of quantum chromodynamics (QCD). Measurements of jets in relativistic heavy-ion collisions are additionally useful for probing QCD matter in the regime of high densities and temperatures since the partons in the jet evolution interact strongly with the medium. This phenomenon is called jet quenching and is characterized by both jet energy loss and modification of the internal structure of the jet. The ALICE experiment is well suited for studies of jets and their corresponding internal structure due to the high precision tracking system. These proceedings report on an overview of recent ALICE jet results in both pp and Pb–Pb collisions. Results in pp collisions include measurements of generalized angularities of groomed and inclusive jets, a measurement of the Lund jet plane, and a measurement of jet axis differences. Results from Pb–Pb collisions include measurements of jet splittings, studies of subjet fragmentation, as well as a measurement of the jet nuclear modification factor made with machine learning techniques. These new results, when combined with the corresponding theoretical comparisons, provide information regarding the QCD processes of the parton shower and hadronization, as well as the underlying physics of jet quenching.

Keywords: Nuclear Physics, Heavy-Ion Collisions, Quark-Gluon Plasma, QCD, Jet Quenching, Jet Substructure

1. Introduction

In hard scatterings, partons scatter off from one another with a high momentum transfer. These partons then fragment and hadronize into a collimated spray of particles called a *jet*. The production of these high-p_{T} partons is calculable in perturbative QCD (pQCD). Jets are sensitive to physics information across many physics scales, from the hard scattering scale to the hadronization scale, a characteristics that makes jets a useful experimental probe of these various processes. Final state particles of the jet are reconstructed via tracking and calorimetry and are reclustered to form an experimental jet using infrared and collinear safe jet clustering algorithms [1] with a specified resolution parameter, related to the cone radius R.

However, jets are not a perfect proxy for the dynamics of the parent parton. Different effects can move energy into or outside of the experimental jet cone, this can happen for instance via emission of partons out of the jet cone during the process of parton showering. Similarly, the hadronization process can also cause energy to move outside of the jet cone. The underlying event (UE), which is formed by particles produced by other processes independent of the hard scattering, additionally moves energy into the jet cone. Effects such as hardonization and the UE cannot be described by pQCD and are therefore *non-perturbative*. Each of these effects has an impact on the resulting jet energy which scales with the cone radius R [2]. Hence, jet measurements can also be used to study these effects.

There are many common uses of jet measurements that will be discussed in this proceedings. Measurements of jets and their substructure have been used

*Mini-Review talk presented at QCD21, 24th High Energy Physics International Conference in QCD (5-9/7/2021, Montpellier - FR).

**PhD Candidate at Yale University

Email address: hannah.bossi@cern.ch (Hannah Bossi for the ALICE Collaboration)

https://doi.org/10.1016/j.nuclphysbps.2022.09.006

in many areas of high energy physics. These proceedings will focus on the use of jet and jet substructure techniques for testing both perturbative and non-perturbative effects of fundamental QCD in pp collisions and investigating the modification of jets and their substructure in Pb–Pb collisions. Overall, jet measurements provide a wealth of physics information.

2. The ALICE Detector

These proceedings focus on jet measurements made with the ALICE detector [3], a dedicated heavy-ion experiment at the Large Hadron Collider. ALICE reconstructs jets at mid-rapidity ($|\eta_{\rm jet}| < 0.7$) in pp, p–Pb and Pb–Pb collisions and utilizes high precision tracking detectors to measure charged particles having $p_{\rm T}$ larger than 150 MeV/c. Full jets, which are jets composed of both charged and neutral constituents, combine charged information from the tracking detectors with the information from the electromagnetic calorimeter, referred to as neutrals but mainly photons from π^0 decays. ALICE is, thus, well-suited for jet measurements, especially measurements of jet substructure.

3. Jet Measurements in pp Collisions

The first category of jet measurements discussed in this proceedings are jet measurements made in pp collisions. ALICE has recently measured the difference between different jet axis definitions in pp collisions. The standard way to define the jet axis is the jet axis found with the anti-$k_{\rm T}$ clustering algorithm [1] with the E-scheme recombination scheme. The jet axis can also be defined by the groomed jet axis, which corresponds to the axis of a jet which has been groomed with the Soft Drop algorithm [4]. The groomed jet axis is less sensitive to soft radiation than the standard axis. Therefore, this observable offers a calculable way to study non-perturbative effects such as hadronization and the UE [5]. The difference between the standard and the groomed jet axis is shown for different grooming parameters in Figure 1. As expected, distributions with more aggressive grooming parameters exhibit a higher probability for misalignment. Ratios to Monte-Carlo (MC) distributions exhibit some differences from data for the standard vs. groomed axes. These deviations are therefore useful for the future tuning of MCs.

ALICE has also recently performed a measurement of the primary Lund jet plane in pp collisions [6]. The Lund jet plane is a two dimensional representation of the phase space of jet splittings in terms of the angle and

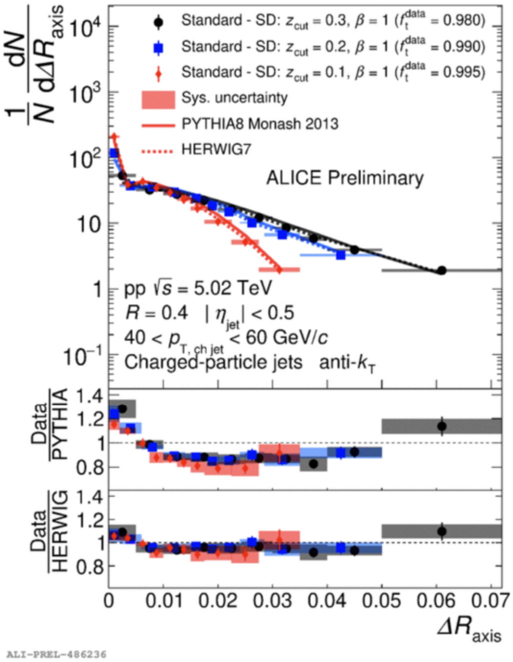

Figure 1: Standard − groomed jet-axis differences for jets with 40 < $p^{\rm ch.}_{\rm T,jet}$ < 60 GeV/c. Comparisons are made with MC events simulated using PYTHIA8 (solid lines) [7] and HERWIG7 (dashed lines) [8], with the ratios to data shown in the bottom two panels. The Soft Drop grooming parameter β is fixed at 1 and $z_{\rm cut}$ is varied from 0.1 to 0.3.

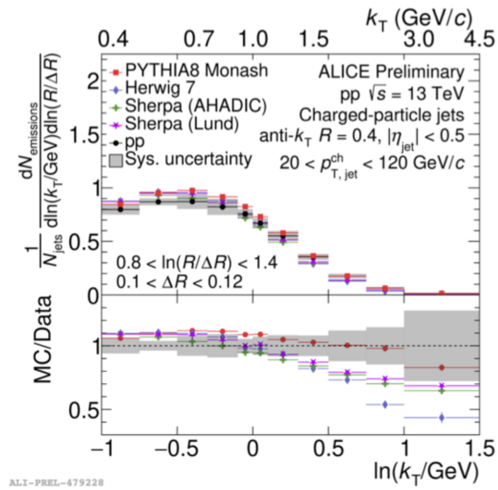

Figure 2: The projections of the primary Lund plane density onto the ln($k_{\rm T}$) axes compared to different MC generators for the region of the Lund jet plane where 0.8 < ln($R/\Delta R$) < 1.4 and 0.1 < ΔR < 0.12. The MC generators shown are PYTHIA8 Monash [7], Herwig 7 [8], and Sherpa 2.2.8 [11] with both the cluster-like hadronization (AHADIC) and string-like hadronization (Lund). The ratios to generators are shown in the bottom panel.

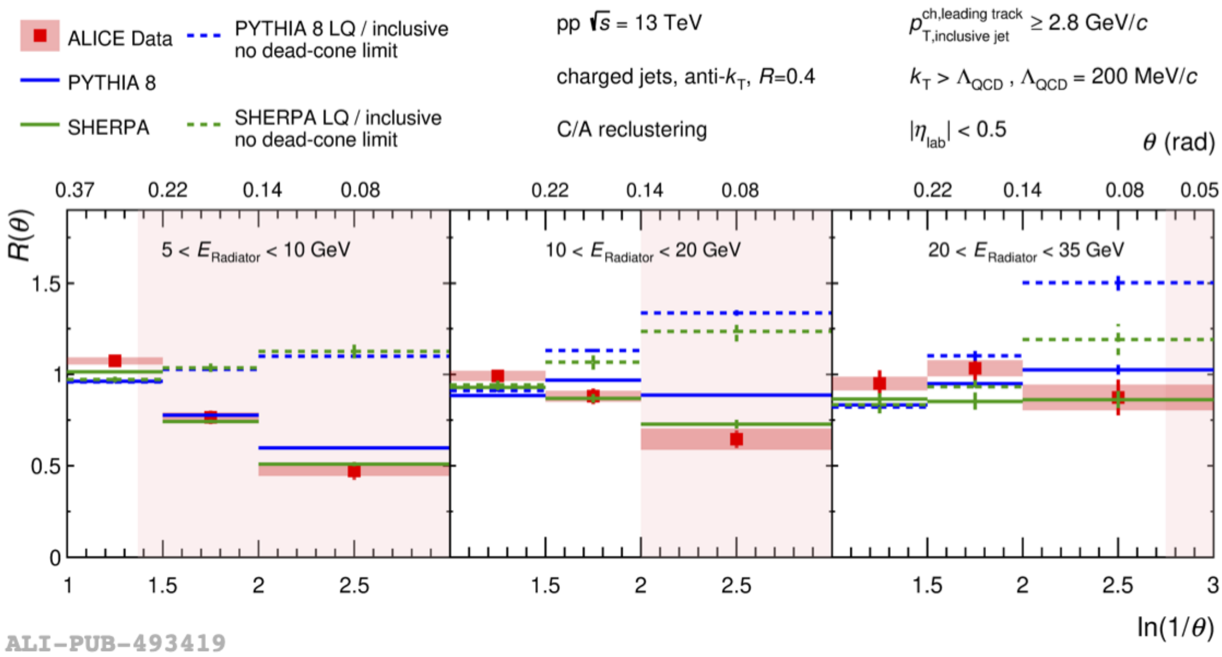

Figure 3: Ratio of the splitting angle probability distribution for D^0 tagged jets as compared to inclusive jets $R(\theta)$ shown for different values of E_{radiator} in each of the panels. Comparisons to PYTHIA and SHERPA simulations are also shown. The red shaded area indicates the angles suppressed by the dead-cone effect assuming a charm quark mass of 1.275 GeV/c^2. Taken from Ref. [9].

momentum fraction of the split. The primary Lund jet plane refers to the Lund plane filled with the emissions from the hardest prong. At leading order the emissions populate the Lund jet plane uniformly, meaning that the running of the coupling will sculpt the plane. Additionally, different regions of the Lund jet plane are sensitive to both perturbative and non-perturbative effects. For this reason, it is interesting to look at projections of the Lund jet plane onto its axes in these various regions and make comparisons to theory. The projection of the primary Lund jet plane in a region of collimated splittings is shown in Figure 2, where there is definite tension between the data and models for the hard collimated splittings in the perturbative region ($k_T > 1$ GeV/c).

Projections of the heavy quark Lund plane were also recently used in the first experimental observation of the dead-cone effect [9]. The dead-cone effect [10] arises from the fact that the pattern of the parton shower is expected to depend on the mass of the initiating parton. Therefore, the gluon spectrum emitted from a heavy quark is expected to be suppressed within a cone of m/E of the emitter. Projections of the heavy-quark Lund plane, shown in Figure 3, reveal suppression of splittings at low angles for the D^0 radiator in D^0 tagged jets as compared to inclusive jets, indicative of the dead-cone effect.

4. Jet Measurements in Pb–Pb Collisions

In heavy-ion collisions, jets are predominantly used as a probe of the QGP medium formed in these collisions. The hard-scattered high-p_T parton interacts with the QGP resulting in jet energy loss and substructure modification. Jets serve as an excellent probe of the QGP as they are formed early in the collision before QGP formation, therefore experiencing its full evolution. Conveniently, jets measured in pp collisions can serve as a reference representing a vacuum-like case, where no QGP is present. Jet measurements in heavy-ion collisions are made difficult due to the large UE which shifts and smears the jet energy scale by significant energy comparable to the jet energy itself, particularly at larger R and lower in p_T.

The conventional approach in ALICE to address the large UE contributions is to first apply a minimum p_T requirement on the leading track of the jet, then correct the jet with a pedestal-based subtraction of the mean underlying event p_T density in given event (ρ). Mathematically, this is given as

$$p_{T,\text{jet}}^{\text{corr}} = p_{T,\text{jet}}^{\text{raw}} - \rho \cdot A_{\text{jet}}, \tag{1}$$

where A_{jet} is the jet area and $p_{T,\text{jet}}^{\text{raw}}$ is the uncorrected jet p_T.

Recently, a novel machine learning approach [12] has been used in order to correct jets for the background particles that overlay them. This approach utilizes a shallow neural network to create a mapping from jet properties (including properties of the constituents of the jet) to $p_{\mathrm{T,jet}}^{\mathrm{corr}}$, which is less affected by fluctuations. Following this correction, there are still some residual fluctuations and detector effects remaining, which need to be corrected for in an unfolding procedure.

This ML-based method was then utilized in order to perform a measurement of the nuclear modification factor (R_{AA}) [13]. The R_{AA} is designed to quantify the expectation from jet energy loss that jet yields will be suppressed (as compared to the vacuum case) at a given p_{T}. Mathematically, the R_{AA} is given as

$$R_{\mathrm{AA}} = \frac{\frac{1}{N_{\mathrm{event}}} \frac{\mathrm{d}^2 N_{\mathrm{jet}}^{\mathrm{PbPb}}|_{\mathrm{cent}}}{\mathrm{d}p_{\mathrm{T}}\mathrm{d}y}}{\langle T_{\mathrm{AA}} \rangle \frac{\mathrm{d}^2 \sigma_{\mathrm{jet}}^{\mathrm{pp}}}{\mathrm{d}p_{\mathrm{T}}\mathrm{d}y}}. \quad (2)$$

When this ratio is less than 1, this is indicative of jet suppression and is consistent with expectations of QGP formation. The result of the application of the ML-based approach as compared to the conventional area-based (AB) approach (as defined in Equation 1) is shown in Figure 4. Jet suppression is observed down to 40 GeV/c, a significant extension of the low p_{T} reach compared to the area-based approach.

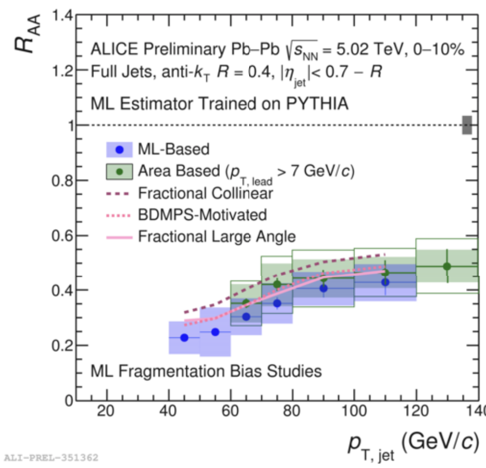

Figure 4: The R_{AA} with the ML and AB method are shown for R = 0.4 jets in 0–10% Pb–Pb collisions. The R_{AA} are compared to the fragmentation bias curves for a toy model with three different modifications.

The fragmentation bias introduced by utilizing constituent information from PYTHIA jets in training was also explored. This was done by making three different toy modifications to the constituents of the jet, then training on this modified sample, measuring the resulting bias. The ML-based result is relatively robust to the explored biases as shown in Figure 4.

Jet splittings are also measured in heavy-ion collisions with the goal of probing the extent to which the colored QGP medium resolves the color structure of the jet. If the interactions with the medium are decoherent, the jet splittings will be resolved by the medium and the two prongs will lose energy as two separate objects, representing an increase in overall energy loss. In the fully decoherent case, this corresponds to a resolution length in the plasma of $L_{\mathrm{res}} = 0$. If the interactions with the medium are coherent, the jet splittings will not be resolved by the medium, resulting in less energy loss. The fully coherent case corresponds to an infinite resolution length $L_{\mathrm{res}} = \infty$.

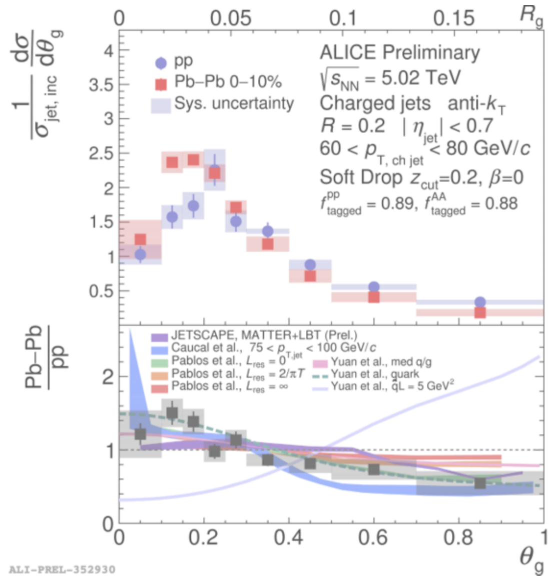

Figure 5: Unfolded θ_{g} distributions for charged-particle jets in 0–10% central Pb–Pb collisions compared to pp collisions for R = 0.2. The ratios in the bottom panel are also compared to theoretical predictions [14–17].

Due to the large background in heavy-ion collisions, jet splittings are often groomed with a Soft Drop grooming procedure [4] in order to remove softer background contributions and access the hard parton splittings. ALICE has measured fully-corrected groomed jet splittings in Pb–Pb collisions for the first time [18]. The unfolded θ_{g} distributions, corresponding to the groomed angular scale of the splitting, are shown in Figure 5. Here, a suppression of wide angle splittings is observed. This suppression is favored by models including decoherence effects. However, a similar effect could also be observed in a coherent picture with a high quark fraction. There-

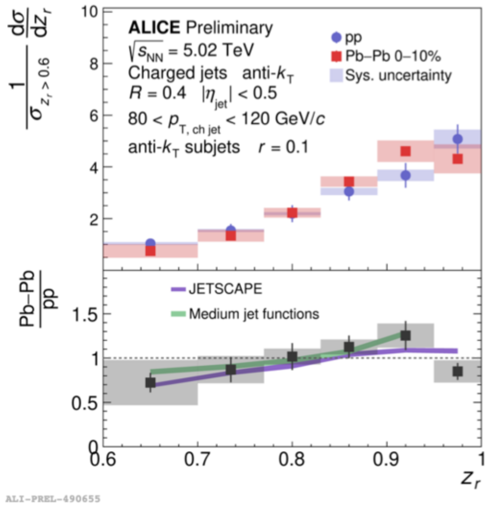

Figure 6: The z_r results in Pb–Pb compared to pp for $R = 0.4$ with $r = 0.1$. The ratio in the bottom panel additionally includes comparisons to theoretical predictions from JETSCAPE[17] and in-medium jet functions [19–21].

fore, further measurements will be needed to disentangle the potential (de)coherence of the QGP medium.

Additionally, ALICE has performed the first measurement of the subjet fragmentation function, which measures the fragmentation of subjets with radius r within a jet of radius R where $R > r$. The fragmentation pattern is defined with a variable z_r where

$$z_r = \frac{p_{T,subjet}}{p_{T,jet}}. \tag{3}$$

These distributions were measured for $R = 0.4$ jets with various values of r in both pp and Pb–Pb collisions, where the modification between the two systems is of physical interest. The z_r distributions for $R = 0.4$ and $r = 0.1$ are shown in Figure 6, where there is a hint of hardening at intermediate z_r and subsequent modification as $z_r \to 1$. In this region, the sample is close to a purely quark jet sample, meaning that a modification of the quark and gluon fractions could also play a role in these results.

5. Conclusions

In conclusion, jets offer a wealth of experimental observables that aim to investigate many different physics questions. ALICE is well suited to make such measurements of jets and their substructure at low/intermediate p_T at the LHC. Recent ALICE jet measurements report new discriminative observables which can be measured differentially. Such differential measurements have shown great promise in isolating different effects and making new insights into fundamental mysteries of QCD.

References

[1] M. Cacciari, G. P. Salam and G. Soyez, JHEP **04**, 063 (2008) doi:10.1088/1126-6708/2008/04/063 [arXiv:0802.1189 [hep-ph]].
[2] A. M. Sirunyan *et al.* [CMS], JHEP **12**, 082 (2020) doi:10.1007/JHEP12(2020)082 [arXiv:2005.05159 [hep-ex]].
[3] B. B. Abelev *et al.* [ALICE], Int. J. Mod. Phys. A **29**, 1430044 (2014) doi:10.1142/S0217751X14300440 [arXiv:1402.4476 [nucl-ex]].
[4] A. J. Larkoski, S. Marzani, G. Soyez and J. Thaler, JHEP **05**, 146 (2014) doi:10.1007/JHEP05(2014)146 [arXiv:1402.2657 [hep-ph]].
[5] P. Cal, D. Neill, F. Ringer and W. J. Waalewijn, JHEP **04**, 211 (2020) doi:10.1007/JHEP04(2020)211 [arXiv:1911.06840 [hep-ph]].
[6] S. Acharya *et al.* [ALICE], https://cds.cern.ch/record/2759456
[7] T. Sjostrand, S. Mrenna and P. Z. Skands, Comput. Phys. Commun. **178**, 852-867 (2008) doi:10.1016/j.cpc.2008.01.036 [arXiv:0710.3820 [hep-ph]].
[8] J. Bellm, S. Gieseke, D. Grellscheid, S. Plätzer, M. Rauch, C. Reuschle, P. Richardson, P. Schichtel, M. H. Seymour and A. Siódmok, *et al.* Eur. Phys. J. C **76**, no.4, 196 (2016) doi:10.1140/epjc/s10052-016-4018-8 [arXiv:1512.01178 [hep-ph]].
[9] S. Acharya *et al.* [ALICE], [arXiv:2106.05713 [nucl-ex]].
[10] Y. L. Dokshitzer, V. A. Khoze and S. I. Troian, J. Phys. G **17**, 1602-1604 (1991) doi:10.1088/0954-3899/17/10/023
[11] T. Gleisberg, S. Hoeche, F. Krauss, M. Schonherr, S. Schumann, F. Siegert and J. Winter, JHEP **02**, 007 (2009) doi:10.1088/1126-6708/2009/02/007 [arXiv:0811.4622 [hep-ph]].
[12] R. Haake and C. Loizides, Phys. Rev. C **99**, no.6, 064904 (2019) doi:10.1103/PhysRevC.99.064904 [arXiv:1810.06324 [nucl-ex]].
[13] H. Bossi [ALICE], [arXiv:2009.02269 [nucl-ex]].
[14] J. Casalderrey-Solana, G. Milhano, D. Pablos and K. Rajagopal, JHEP **01**, 044 (2020) doi:10.1007/JHEP01(2020)044 [arXiv:1907.11248 [hep-ph]].
[15] F. Ringer, B. W. Xiao and F. Yuan, Phys. Lett. B **808**, 135634 (2020) doi:10.1016/j.physletb.2020.135634 [arXiv:1907.12541 [hep-ph]].
[16] P. Caucal, E. Iancu and G. Soyez, JHEP **10**, 273 (2019) doi:10.1007/JHEP10(2019)273 [arXiv:1907.04866 [hep-ph]].
[17] J. H. Putschke, K. Kauder, E. Khalaj, A. Angerami, S. A. Bass, S. Cao, J. Coleman, L. Cunqueiro, T. Dai and L. Du, *et al.* [arXiv:1903.07706 [nucl-th]].
[18] S. Acharya *et al.* [ALICE], [arXiv:2107.12984 [nucl-ex]].
[19] J. W. Qiu, F. Ringer, N. Sato and P. Zurita, Phys. Rev. Lett. **122**, no.25, 252301 (2019) doi:10.1103/PhysRevLett.122.252301 [arXiv:1903.01993 [hep-ph]].
[20] D. Neill, F. Ringer and N. Sato, JHEP **07**, 041 (2021) doi:10.1007/JHEP07(2021)041 [arXiv:2103.16573 [hep-ph]].
[21] Z. B. Kang, F. Ringer and W. J. Waalewijn, JHEP **07**, 064 (2017) doi:10.1007/JHEP07(2017)064 [arXiv:1705.05375 [hep-ph]].